International Journal of Pharmaceutics, 57 (1989) 95–105
Elsevier

IJP 01929

Characterization of the viscoelastic properties of compacted pharmaceutical powders by a novel nondestructive technique

Galen W. Radebaugh [2], Suresh R. Babu [1] and Joseph N. Bondi [1]

[1] *McNeil Consumer Products Co., Research and Development, Camp Hill Road, Ft. Washington, PA 19034 and* [2] *Parke-Davis Pharmaceutical Research, Warner-Lambert Co., 170 Tabor Road, Morris Plains, NJ 07950 (U.S.A.)*

(Received 17 February 1989)
(Modified version received 15 June 1989)
(Accepted 16 June 1989)

Key words: Viscoelasticity; Elastic modulus; Viscous modulus; Damping; Porosity; Compression; Compaction; Powder; Compact; Nondestructive testing

Summary

The mechanical properties of a compact are typically measured by destructive tests that examine the mechanical failure properties of compacts. These tests result in irreversible damage to the mechanical structure of the compact and consequently provide little information about viscoelastic properties. This report describes a novel nondestructive technique capable of measuring the viscoelastic properties of compacted powders without fracture or permanent deformation of the compact. The technique uses small strain sinusoidal oscillatory torsion of rectangularly shaped compacts. The fundamental viscoelastic parameters of elastic modulus, G', viscous modulus, G'', and damping, tan δ, are determined as a function of strain, rate of strain, composition, method of manufacture and water content of the compact. With compacts of microcrystalline cellulose as a model, it was found that viscoelastic parameters can provide insight into the processes that result in bonding and structure formation. In particular, the magnitude of G' for microcrystalline cellulose was found to be similar to G' of amorphous polymers in the glassy state, but one to two decades less than the G' of crystalline solids. Findings support the rationale that van der Waals' forces are the primary origin of bonding between particles. A relation was found between reciprocal porosity of the compact and G', illustrating rearrangement and consolidation mechanisms in addition to bonding mechanisms after an intact compact had already been formed. It was also shown that G' could differentiate the influence of water content, above and below an amount corresponding to one molecule of water per sorption site, on bond formation and bond integrity in a formed compact.

Introduction

The compaction of pharmaceutical powders into tablets remains a preferred method of manufacturing dosage forms. Usually, the compaction properties of a powder are measured by destructive tests that examine the mechanical failure properties of compacts. In a development or manufacturing setting, mechanical properties are typically measured with a tablet breaking strength tester (Brook and Marshall, 1968; Goodhart et al., 1973). These testers are commonly referred to as hardness testers, but the test they perform could be more accurately described as a type of diametral compression that measures radial tensile strength (Carstensen, 1977). Complicated variable fracture patterns often lead to inaccurate results.

Correspondence: G.W. Radebaugh, Parke-Davis Pharmaceutical Research, Warner-Lambert Co., 170 Tabor Rd, Morris Plains, NJ 07950, U.S.A.

In a laboratory setting, radial tensile strength can be more reproducibly measured when test conditions are carefully controlled such that tablets show normal failure (Fell and Newton, 1968, 1970). Hiestand and Smith (1984) reported the transverse compression of square compacts between platens narrower than the compact provides more reproducible results. It has also been suggested that axial tensile strength be measured since this measurement is not as sensitive to crack propagation (Nystrom et al., 1977; Jarosz and Parrott, 1982).

Another destructive test, the flexure test operates by bending a compacted rectangular beam until failure. It can be used for determining tensile strength because tablets invariably fail in tension as evidenced by splitting into halves (David and Augsburger, 1974; Mashadi and Newton, 1987). Other destructive tests also include surface hardness measurements as determined by static or dynamic indentation methods. Surface hardness tests are sometimes referred to as nondestructive, because the compacts do not break apart during the test. Even so, the tests do result in the formation of a permanent indentation on the surface of the compact (Hiestand and Smith, 1984; Jetzer et al., 1985).

Even though the above tests determine mechanical properties by a variety of mechanisms, each results in irreversible damage to the mechanical structure of the compact. Consequently, limited information can be learned about the viscoelastic mechanical properties of the compact. Compacts though solid, exhibit two phenomena when subjected to deformation: spontaneously reversible deformation called elasticity and irreversible deformation called flow. Hence, compacts can be rheologically classified as viscoelastic. This has been demonstrated by Rippie and Danielson (1981) and Danielson et al. (1983) where the viscoelastic behavior of compacts has been studied by measuring stress-relaxation phenomena during the unloading and post-compression periods in the die of a rotary tablet press. These authors postulated viscoelastic parameters can provide insight into kinetically controlled changes in structure.

Ideally, viscoelastic properties should be determined by nondestructive tests such that the structure one is attempting to measure is not destroyed. This report describes a new nondestructive technique capable of measuring the viscoelastic properties of compacted pharmaceutical powders without fracture or permanent deformation of the compact. The technique utilizes forced small strain sinusoidal oscillatory torsion of rectangular compacts. The fundamental viscoelastic parameters of elastic modulus, G', viscous modulus, G'', and damping, tan δ, are determined as a function of strain, rate of strain (frequency of torsion), composition and method of manufacture of the compact. Each compact remains intact after the test and can be retested. Most significantly, this report illustrates the utility of nondestructive viscoelastic parameters as an aid in the interpretation of powder compaction data.

Materials and Methods

Materials

The powder used to produce all compacts was microcrystalline cellulose (Avicel PH102, lot 8402397, FMC Corp., Philadelphia, PA). Water content of the powder and compacts made from the powder was determined by titrimetry (Mitsubishi moisture analyzer, model CA-05, Mitsubishi, Tokyo) prior to compaction. The true density of the powders was determined with an air comparison pycnometer (model 930, Beckman Instruments, Fullerton, CA) and found to be 1.58 g/cm^3 (appendix I).

Sample preparation

Rectangularly shaped compacts (122 × 50 × 2.8 mm) were prepared with a hydraulic press (model M, Fred S. Carver, Inc., Menononee Falls, WI) and a custom designed split die and yolk assembly that provided triaxial decompression. The design of the split die and yolk assembly was similar to that described by Hiestand and Smith (1984). The thickness of the compacts was controlled by placing mechanical stops on the hydraulic press so the upper and lower punches would be 2.8 mm apart upon maximum punch penetration. Powder was evenly layered into the bottom of the die cavity to ensure uniform distribution of the compression force. Since all compacts were compressed to a

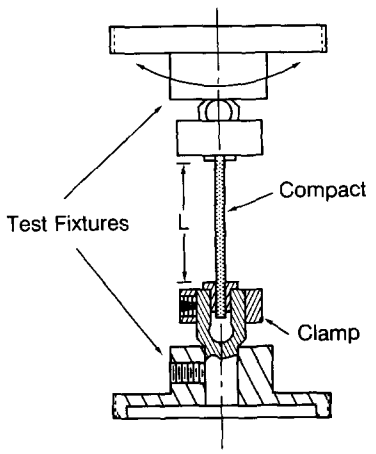

Fig. 1. Side cross-sectional view of a compact mounted between the upper and lower test fixtures. The effective dimensions of the mounted compact between the fixtures were 2.8 × 12.3 × 33.0 mm.

constant thickness of 2.8 mm, porosity, ϵ, could be varied by changing the weight of powder placed in the die cavity.

Test equipment

The viscoelastic properties of the compacts were measured with a dynamic mechanical tester (dynamic spectrometer, model RDS-7700, Rheometrics, Inc., Piscataway, NJ). The spectrometer subjected the compacts to forced small strain sinusoidal oscillations in torsion. The rectangular shaped compacts were mounted on end between two stainless steel test fixtures such that each end was clamped in place (Fig. 1). The upper fixture was driven by a motor, which in turn was commanded by a computer to oscillate at a prescribed frequency (rate of strain) and amplitude (strain). Stresses induced in the compact were transmitted through the lower test fixture to a torque detecting transducer where deflections were converted to electrical signals and relayed to a phase analyzer. The phase analyzer then resolved the signals into elastic and viscous components of the complex modulus and the phase angle between them. Calculations for the dynamic moduli of G' and G'' in terms of dyn/cm^2 were accomplished with a personal computer (IBM PC-AT) and proprietary software (RECAP-2 analysis program, Rheometrics).

Description of experiments

All tests were made at the controlled temperature of $22 \pm 0.5\,^{\circ}$C. Samples were oscillated over the range of strain, γ, from 0.01 to 0.1%, and over the range of frequency, ν, from 0.63 to 630 Hz. The elastic modulus, G', viscous modulus, G'', and damping, tan δ, were calculated for each sample at each ν and γ.

Theoretical

Linear viscoelasticity and the calculation of dynamic moduli for forced torsion of a rectangular compact

In a dynamic experiment, under strains within a sample's range of linear viscoelasticity, the maximum magnitude of stress, σ_0, the maximum magnitude of strain, γ_0, and the phase angle between stress and strain, δ, are related to moduli by the following expression (Radebaugh and Simonelli, 1983):

$$G^* = (\sigma_0/\gamma_0)\cos\delta + i(\sigma_0/\gamma_0)\sin\delta \tag{1}$$

where

$$G' = (\sigma_0/\gamma_0)\cos\delta \tag{2}$$

and

$$G'' = (\sigma_0/\gamma_0)\sin\delta \tag{3}$$

where G^* is the complex modulus.

It can also be shown that

$$2\pi \tan\delta = 2\pi(G''/G') = \Delta W/W \tag{4}$$

where $\Delta W/W$ is the ratio of the energy dissipated per cycle of deformation divided by maximum energy stored per cycle of deformation. Hence, G' is often referred to as the storage modulus because it indicates the amount of energy stored elastically upon deformation, and G'' is often referred to as the loss modulus because it indicates the amount of energy lost to viscous dissipation.

In forced torsion of a rectangular compact, the peak magnitude of the torque detected by the transducer is a measurement of the total stress

required to deform the compact. The geometrical form factor for torsion of a rectangular sample with the dynamic spectrometer is:

$$k = L/\{t^3 w[(1/3) - 0.21(t/w)]\} \quad (5)$$

where L is the length of the sample between the clamps, t is the thickness and w is the width. If inertial effects are assumed negligible, the maximum stress is expressed as:

$$\sigma_0 = M/\{t^2 w[(1/3) - 0.21(t/w)]\} \quad (6)$$

and the maximum strain is:

$$\gamma_0 = \alpha t/L \quad (7)$$

where M is the torque and α is the angular displacement. The combination of Eqns. 5–7 with Eqns. 2 and 3 gives:

$$G'(\text{dyn/cm}^2) = (kM/\alpha)\cos\delta \quad (8)$$

and

$$G''(\text{dyn/cm}^2) = (kM/\alpha)\sin\delta. \quad (9)$$

Therefore,

$$G''/G' = \sin\delta/\cos\delta = \tan\delta. \quad (10)$$

Results and Discussion

Effects of strain on linear viscoelasticity and compact integrity

The relationship between G' and γ was examined by subjecting compacts to a complete decade of strain, from 0.01 to 0.1%. The results of a typical experiment for compacts of microcrystalline cellulose, compressed and compacted to a ϵ of 0.195, from powder with 3.5% w/w water content, are illustrated in Table 1. The significance of the data is three-fold. First, viscoelastic behavior is linear and the assumptions of linearity used to derive the equations for G', G'', and tan δ are valid, because there is little change in G' over the entire range of γ examined. Second, the data shows the compacts retained their integrity by not fracturing under the conditions of strain in these studies. Last, the data illustrates the ability to obtain good reproducibility from compact to compact and experiment to experiment.

TABLE 1

Effect of strain on the elastic modulus of compacts of microcrystalline cellulose with a porosity of 0.195, and at a torsional frequency of 1.0 Hz

The average and standard deviation were calculated from the data obtained for six compacts.

Strain (γ) (10^{-2}%)	Elastic modulus (G') (10^{10} dyn/cm^2)			
	x	S.D.	max.	min.
1.0	1.43	0.048	1.49	1.36
2.0	1.43	0.041	1.49	1.38
3.0	1.44	0.048	1.51	1.38
4.0	1.45	0.047	1.52	1.39
5.0	1.45	0.047	1.52	1.39
6.0	1.45	0.047	1.52	1.39
7.0	1.44	0.049	1.51	1.38
8.0	1.44	0.049	1.51	1.38
9.0	1.43	0.050	1.51	1.38
10.0	1.43	0.052	1.51	1.37

Effects of rate of strain on viscoelastic properties

In Fig. 2 it can be seen there is an increase in G' as the compacts are oscillated starting at a frequency of 0.63 Hz and increasing up to a frequency of 630 Hz. Even though the total change is relatively small, the change is more rapid during the first decade of change of frequency and asymptotes during the last decade of frequency. Modulus data is typically plotted on the log scale because significant mechanical changes in polymers usually result in multiple decades of change in modulus. So, practically speaking, a change in G' from about 1.3×10^{10} to 1.6×10^{10} dyn/cm^2, though measurable, does not indicate significant mechanical changes within a system. Even so, the phenomena can be explained in terms of molecular changes within the compact.

When frequency is low, molecules are apt to rearrange themselves within the time scale of straining thereby diminishing elastic deformation

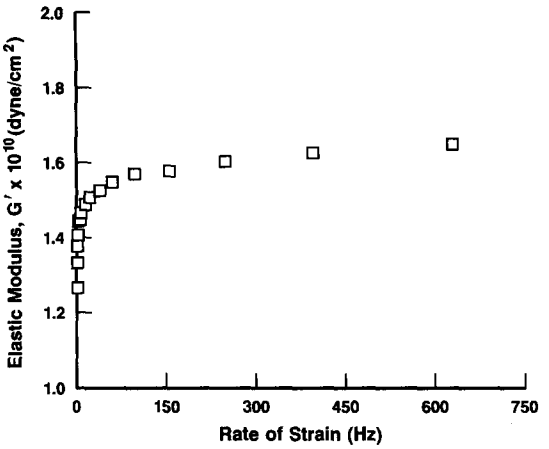

Fig. 2. Plot of elastic modulus (G') vs rate of strain (frequency of torsion) for compacts of microcrystalline cellulose, at a porosity of 0.195, 0.01% strain and 22°C. Each point represents the average of determinations from six compacts. Standard deviation at each frequency ranged from 0.05 to 0.06×10^{10} dyn/cm^2.

and G'. Increases in frequency increase elastic deformation and thereby G'. At frequencies where G' asymptotes, it can be concluded that the molecular chains of the microcrystalline cellulose are not able to rearrange themselves at all during the time of straining the compacted sample. For amorphous polymeric materials, this phenomenon is characteristic of the glassy state, where G' asymptotes to a limiting modulus, G_E (Aklonis and MacKnight, 1983). At temperatures where the glassy state occurs, molecules appear frozen and the only deformation is by distortion of primary and secondary bonds and bond angles.

The magnitude of the limiting modulus is primarily determined by true elastic deformation arising from the straining of intermolecular bonds (van der Waals) and from the flexing of main chain bonds. Such phenomena are characteristic of amorphous polymers where the polymer chains are intimately intertwined. It is interesting to note that the magnitude of the limiting modulus as shown in Fig. 1 (about 10^{10} dyn/cm^2) is comparable to the G_E of polymers with effectively high molecular weight ($> 10^4$). The molecular weight of microcrystalline cellulose is approx. 36 000 (Am. Pharm. Assoc., 1986). Barlow and Lamb (1959) collected data for G_E for a variety of polymers in the glassy state and found most values to be within a factor of two of 2×10^{10} dyn/cm^2. Apparently, G_E for high polymers does not vary greatly with structure. This explains the rationale that the straining of van der Waals' bonds and flexing of main chain bonds are the origin of elastic deformation, and these features are relatively independent of structure.

For microcrystalline cellulose though, elastic deformation is also subject to the constraints of a crystal lattice, since it is approx. 80% crystalline (Durbetaki and Quail, 1982). Consequently, the elastic modulus results from the sum of the contributions of van der Waals' forces, hydrogen bonds and constraints of the crystal lattice. The limiting modulus of a typical crystalline solid is between 10^{11} and 10^{12} dyn/cm^2. Since the limiting modulus depicted in Fig. 2 is approx. 10^{10}, it can be assumed that the 10–100-fold reduction in modulus from that of a typical crystalline solid is due in part to the amorphous component of microcrystalline cellulose and in part to the porosity in the compact. Porosity not only exists between particles, but potentially also within particles. If it is assumed that the quantity and quality of bonds is proportional to areas of true contact between particles, then by inference the quantity and quality of bonds is inversely proportional to the porosity of the compact. Hence, the observed limiting modulus of microcrystalline cellulose compacts results from the contributions of chemical composition, chemical structure, porosity, and the quantity and quality of bonds between particles.

Density-modulus relationships

The mechanical properties of compacts are often characterized as a function of porosity. Porosity is a measure of the void space within the compact and is related to density by

$$\epsilon = 1 - (\rho_c/\rho) = 1 - D \qquad (11)$$

where ρ_c is the apparent density of the compact, ρ is the true density of the powder, and the ratio of ρ_c/ρ is the relative density of the compact, D (Carstensen, 1977).

Intuitively, the mechanical properties of a compact are a function of the mechanical properties of

the powder itself, the arrangement of particles, and the degree of interparticle bonding. The degree of interparticle bonding would be expected to increase as the amount of porosity decreases because more areas of true contact between particles can form. Therefore, porosity is inversely proportional to bonding. As the porosity of the compact approaches zero, one would expect the moduli of the compact to approach the moduli of non-porous powder.

Rule of mixtures for the prediction of the viscoelastic properties of composite materials

It is typical for polymeric composite systems formed by melt or casting processes to follow a generalized modulus equation known as the 'rule of mixtures' (Nielsen, 1974). A composite, which is also referred to as a filled system, is defined as a material with a continuous matrix phase and a discontinuous filler phase. The filler phase can be solid, liquid or gas. It is written as

$$G' = G_1'\phi_1 + G_2'\phi_2 \tag{12}$$

where G' is the elastic modulus of the filled system, G_1' is the elastic modulus of the pure matrix phase, G_2' is the elastic modulus of the filler phase, and ϕ_1 and ϕ_2 are the volume fractions of the matrix phase and the filler phase respectively. For compacted polymeric materials where the filler is gaseous void space, ϕ_2 is equal to ϵ and $G_2'\phi_2$ is equal to zero, since G' of air is zero. Hence, the elastic modulus of pure powder should be predicted by

$$G' = G_1'\phi_1 \tag{13}$$

where ϕ_1 equals $(1 - \phi_2)$ or $(1 - \epsilon)$. Theoretically, G_1' should be constant and a plot of G' vs ϕ_1 should be a straight line.

Fig. 3 shows experimental data for compacts of microcrystalline cellulose from a ϕ_1 of 0.88–0.33 ($\epsilon = 0.12$–0.67). Clearly, the data shows G_1' is not constant. The curve can be divided into two linear portions through which straight lines can be drawn that intersect in the region of ϕ_1 equal to 0.55–0.60. It is this region where a change in mechanical properties occurs. As will be described

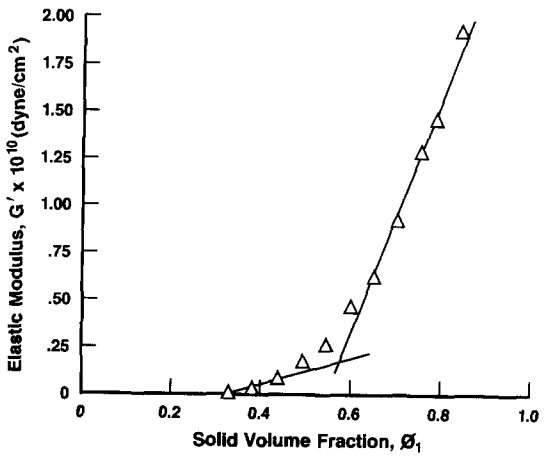

Fig. 3. Plot of elastic modulus (G') vs solid volume fraction (ϕ_1) for compacts of microcrystalline cellulose, at 0.01% strain, 1.0 Hz, and 22°C. Each point represents the average of determinations from six compacts.

in the next section, the mechanical properties of a compact can be assumed to be a function of the sum of the processes (consolidation, rearrangement, plastic deformation, elastic recovery and interparticle bonding) that lead to the formation of the compact. During the process of consolidation, loss of porosity occurs not only between particles but potentially also within particles. A loss of porosity within particles would contribute to an increase in G_1' as ϕ_1 increases. Ideally, G_1' should equal G_0', the elastic modulus of the compact at zero porosity. The value of G_1' calculated from the slope of the linear portion from ϕ_1 of about 0.60–0.88 is approx. 6×10^{10} dyn/cm^2, which is over 6-times the value of G_1' calculated from the slope of the linear portion from ϕ_1 of about 0.33–0.55. The 6-fold increase in G_1' indicates a critical solid fraction was achieved through consolidation and deformation whereby the underlying mechanical structure responsible for viscoelastic properties was altered. One explanation for this change could be the loss of porosity within particles.

Fig. 4 further supports the hypothesis that a significant mechanical change (and hence a change in mechanism) is occurring at ϕ_1 between 0.55 and 0.60. This is evident by the intersection of a decline in tan δ from about 0.4 to 0.55 and the formation of a flat plateau from 0.55 to 0.88. Tan

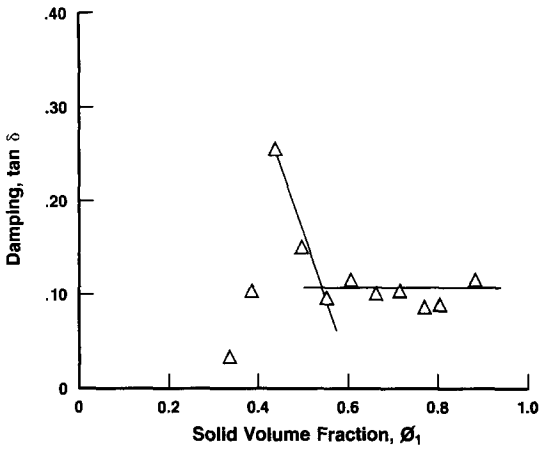

Fig. 4. Plot of damping (tan δ) vs solid volume fraction (ϕ_1) for compacts of microcrystalline cellulose, at 0.01% strain, 1.0 Hz, and 22° C. Each point represents the average of determinations from six compacts.

δ is proportional to G''/G' and is a measure of the energy dissipated to energy stored per cycle of deformation. Even though the role of damping is not well known, it is sensitive to all types of transitions, relaxation processes and the morphology of multiphase systems such as filled or composite materials. Damping is a measure of imperfection in elasticity. An increase in damping means that an increased portion of the energy used to deform a material is dissipated as heat. Newtonian materials are examples of infinite damping where all energy used to deform the material is dissipated as heat. Perfectly elastic materials exhibit no damping because no energy used for deformation is dissipated as heat. It must be noted that Fig. 4 also illustrates a change at ϕ_1 of about 0.45 which is not evident in Fig. 3, indicating changes in structure that affect G'' (energy dissipation) rather than G' (energy storage). This point may signify the end of significant consolidation and rearrangement mechanisms prior to deformation of the particles and loss of intraparticle porosity.

Interpretation of powder compaction data with reciprocal porosity versus elastic modulus plots

Heckel (1961a,b) considered the compression and compaction of powders to be analogous to a first order chemical reaction, where the pores are the reactant and densification can be described by

$$dD/dP = k(1 - D) \tag{14}$$

where D is relative density, $(1 - D)$ is the pore fraction ($(1 - D)$ equals ϵ), P is pressure, and k is a proportionality constant. Development of Eqn. 14 gives

$$\ln(1/(1 - D)) = kP + \ln(1/(1 - D_0)) \tag{15}$$

where D_0 is the relative density at zero pressure. A typical plot of $\ln(1/1 - D))$ vs P shows curvature at low P and linearity at high P. Extrapolation of the linear portion of the plot to P equals zero gives $\ln(1/(1 - D_0))$. The curved or nonlinear portion of the plot was attributed to the effects of rearrangement processes in the powder as individual particles instead of bonding into a coherent mass. The transition from nonlinear to linear was associated with increased interparticle bonding, such that linearity represents densification by plastic deformation of the compact after an appreciable amount of interparticle bonding has taken place.

The compression and compaction of a powder bed can be described by the following sequence of events:

$$\epsilon_A \rightarrow \epsilon_B \rightarrow \epsilon_C \rightarrow \epsilon_D \rightarrow \epsilon_E$$

where each letter represents the state of the powder bed as follows: ϵ_A, loose powder prior to consolidation and rearrangement; ϵ_B, powder that has been compressed and exhibits consolidation and rearrangement but not interparticle bonding; ϵ_c, powder that exhibits consolidation, rearrangement, deformation, and interparticle bonding; ϵ_D, powder undergoing deformation and interparticle bonding; ϵ_E, powder compressed and compacted to a state of zero porosity.

A Heckel plot provides a model for states ϵ_A–ϵ_D but not ϵ_E. It graphically divides the events into only two basic categories. The curved portion models the states of ϵ_A–ϵ_C while the linear portion models the state of ϵ_D.

A plot of $\ln(1/\epsilon)$ vs G' was made for compacts of microcrystalline cellulose and its shape was

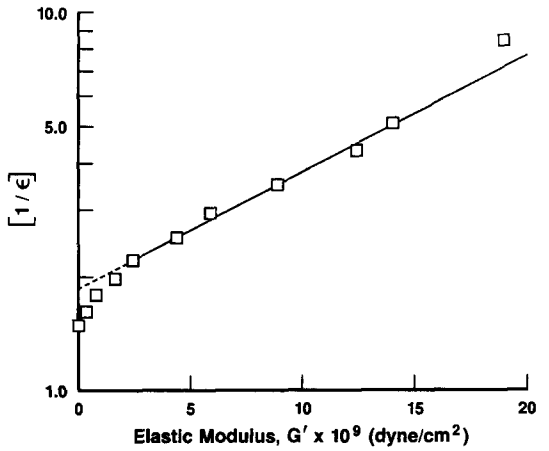

Fig. 5. Semilogarithmic plot of reciprocal porosity ($1/\epsilon$) vs elastic modulus (G') for compacts of microcrystalline cellulose, at 0.01% strain, 1.0 Hz, and 22°C. Each point represents the average of determinations from six compacts.

similar to a typical Heckel plot (Fig. 5). Intuitively, one would expect some form of inverse relationship between ϵ and G' because as ϵ decreases, the number of bonds between particles should increase thereby increasing G' of the compact. The equation for the straight line portion of the curve can be written as:

$$\ln(1/\epsilon) = kG' + \ln(1/\epsilon_0) \qquad (16)$$

where ϵ_0 is the porosity at zero elastic modulus. Even though the 'shapes' of the plots are similar, distinctions must be made in interpretation of the plots because all points in Fig. 5 were obtained from intact compacts. The early curved portion of a Heckel plot is attributed to particles that have not bonded into an intact compact. Unlike Heckel plots, the curved portion of Fig. 5 cannot be attributed to the absence of bonding between particles such that a compact is not formed. This is clear, since all data was generated from intact compacts that retained their integrity throughout the test procedure. Even so, the curved region represents a process of consolidation, deformation and bonding that is different from that which occurs over the linear portion of the plot.

Consequently, the density-modulus relationship depicted in Fig. 5 acts as a model only for the states of ϵ_C–ϵ_D. Since only intact compacts are tested, state ϵ_A is not present. Consequently, the density-modulus relationship provides a greater degree of discernment because the consolidation and rearrangement process without interparticle bonding is omitted from the sequence of events. This allows a cleaner examination of the deformation and interparticle bonding process.

Effect of water content on elastic modulus

In general, it is well known that the water content of pharmaceutical powders affects their ability to be compressed and compacted into a tablet. Powders or granulations that are "too dry" often cap, whereas additional water content can prevent capping and provide for a satisfactory tablet. Zografi (1988) and Zografi et al. (1984, 1986) describe three thermodynamic states of water in microcrystalline cellulose. They are: (1) water directly and tightly bound, with a stoichiometry of one molecule per anhydroglucose unit; (2) water in a relatively unrestricted form; and (3) water in an intermediate state(s), with properties reflecting more structure than bulk water but less structure than tightly bound water. The weight of water sorbed corresponding to one molecule of water per sorption site on the solid is W_m. For microcrystalline cellulose, W_m is about 0.035 g/g. Therefore, water in excess of W_m becomes available to interact with the amorphous and crystalline phases. For example, water has the ability to plasticize many amorphous polymers. Plasticization usually causes measurable changes in viscoelastic properties, making a substance less elastic and more susceptible to compaction.

In this report, the effect of water on the elastic contribution to the viscoelastic properties of compacts of microcrystalline cellulose was examined by two methods. The first method involved preparing all compacts, to a porosity of 0.195 from one lot of microcrystalline cellulose that was conditioned to contain about 6% w/w water. The compacts were then stored in one of a variety of controlled humidity chambers, each at a different relative humidity, until equilibrium was achieved. Representative compacts were analyzed for water content. The compacts were then tested at three different strains and G' was recorded as a function of water content (Fig. 6). The second method

involved preparing compacts to a porosity of 0.195 from different samples of powders that were each equilibrated to a different water content. Powders were analyzed for water content just prior to compaction. The compacts were also tested at three different strains and G' was recorded as a function of water content (Fig. 7).

In Fig. 6 it is apparent that G' is at a plateau from about 1–5% w/w water content, and then begins a steady decline thereafter. An approx. one-third reduction in G' occurs over the range of water content 5–7% w/w. Even though the decline does not begin at 3.5% w/w, this observation is consistent with the hypothesis that a certain amount of water, W_m, is immobilized. Above W_m the water becomes available to interact with the crystalline component and plasticize the amorphous component, thereby lowering G'. Similar to Fig. 6, Fig. 7 also shows a plateau of about 10^{10} dyn/cm^2 at low water content and sudden decline in G' with increasing water content. Unlike the data in Fig. 6 though, the sudden decline begins at about 3.75% w/w water, an amount close to the reported W_m of 0.035 g/g. In addition, G' is reduced by as much as 80% over the range of water content 3.75–8.0% w/w.

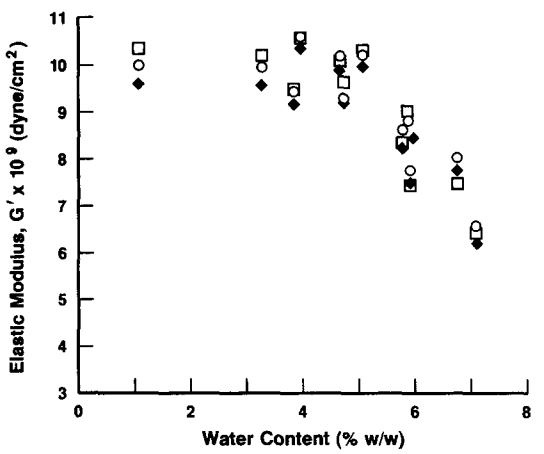

Fig. 6. Plot of elastic modulus (G') vs water content for compacts of microcrystalline cellulose where all compacts were made from powder with a water content of 6% w/w. Compacts were then conditioned to lower or raise the total water content of the compacts. Tests were at 1.0 Hz and 22° C. (□) 0.01% strain, (○) 0.05% strain, (◆) 0.1% strain.

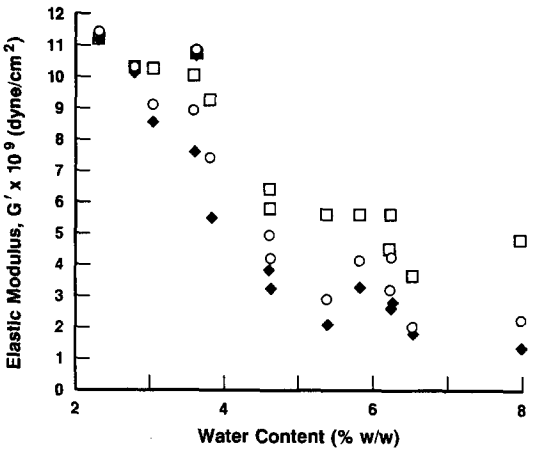

Fig. 7. Plot of elastic modulus (G') vs water content for compacts of microcrystalline cellulose where the powder was conditioned to raise or lower its water content prior to compression and compaction. Resultant compacts were tested at 1.0 Hz and 22° C. (□) 0.01% strain, (○) 0.05% strain, (◆) 0.1% strain.

Due to the experimental conditioning procedures, the powder used to make the compacts in Fig. 7 was plasticized with available water prior to compression and compaction, whereas the compacts in Fig. 6 were plasticized with available water after compression and compaction. The observations in these figures could appear contrary to the generally accepted hypothesis that an increase in plasticity of a powder results in more areas of true contact between particles during compression, and hence a greater degree of bonding and an increase in G'. In all likelihood though, the additional water content has little impact on the ease by which microcrystalline cellulose deforms and forms true areas of contact between particles. Instead, the lowering of G' is probably due to plasticization of the amorphous component of microcrystalline cellulose. The differences between Figs. 6 and 7 can be attributed to the difference in ability of water to distribute itself in noncompressed and noncompacted powder versus compressed and compacted powder.

It must also be noted that significant strain dependence of G' develops at the beginning of the decline in Fig. 7. The lowest strain, 0.01%, gives consistently higher G' than 0.1% strain. Signifi-

cant strain dependence is not evident in Fig. 6. Lower G' with increasing strain implies the existence of time-dependent structural changes, such as the weakening of bonds. It can be deduced that bond integrity is strain dependent at the higher water contents when available water is in the powder prior to compression and compaction. Therefore, the viscoelastic properties of the compacts appear not only a function of water content, but also a function of when the water entered the compact (i.e., pre-compaction or post-compaction). Water appears to distribute itself differently in the powdered state as opposed to the compacted state. Even though the observations in Fig. 7 appear inconsistent with the data in Table 1, that shows little strain dependence, it is important to note that the compacts used to generate the data in Table 1 were made from powder that contained 3.5% w/w water. This level of water content is in the region where strain dependence is just beginning in Fig. 7.

Conclusion

This report has demonstrated a novel nondestructive testing technique that is capable of reproducibly measuring the viscoelastic properties of compacted pharmaceutical powders. Without altering the integrity of the compact, the fundamental parameters of G', G'' and tan δ, can be determined and related to consolidation and compaction mechanisms that occur during compact formation. Interpretation of the parameters, in view of general knowledge about the viscoelastic properties of polymers, can lead to enhanced understanding of interparticle and intraparticle mechanisms of compact formation.

Appendix I

Sample weight and moisture content of microcrystalline cellulose and their effect on density determinations using an air comparison pycnometer

Initial determinations of ρ_{MCC} in our laboratory were approx. 1.75. This contrasted with reported values of 1.56–1.58 g/cm^3 (Nyqvist and Nicklasson, 1983). The instruction manual for the Beckman air comparison pycnometer, model 930, does not specify an optimum sample size for determination of the apparent volume of powders. Hence, the relationship between sample size, measured volume and the resultant calculation of ρ_{MCC} was examined for sample sizes ranging from 0.5 to 9.0 g (Table 2). From sample sizes of 0.5–5.0 g there is a decrease in ρ_{MCC}, but from 5.0 to 9.0 g there is no significant change in ρ_{MCC}. Therefore, the average value of 1.58 g/cm^3 was used for ρ_{MCC}.

TABLE 2

Effect of sample weight on the calculated density of microcrystalline cellulose based on the apparent volume measured with an air comparison pycnometer

Tabulated densities are the average of results from six compacts.

Sample weight (g)	ρ_{MCC} (g/cm^3)	S.D.
0.50	2.40	0.100
1.00	2.22	0.050
2.00	1.74	0.068
3.00	1.68	0.025
4.00	1.64	0.006
5.00	1.59	0.010
6.00	1.59	0.008
7.00	1.58	0.003
8.00	1.57	0.003
9.00	1.58	0.003

TABLE 3

Effect of water content on the calculated density of microcrystalline cellulose based on the apparent volume measured with an air comparison pycnometer

Tabulated densities are the average of results from three six g samples at each level of water content. Different levels of water content were obtained by storing powdered samples in controlled humidity chambers of different humidities.

Water content (% w/w)	ρ_{MCC} (g/cm^3)
1.17	1.56
2.83	1.58
3.66	1.55
4.62	1.58
5.83	1.56
6.24	1.55

The influence of water content on ρ_{MCC} was also examined since the water content of microcrystalline cellulose can vary with storage conditions (Zografi et al., 1984). In addition, Beckman Instruments suggests that materials that interact with atmospheric water vapor may give lower than true volumes and artificially high resultant densities (Beckman Instruments, 1977). Densities calculated from samples containing 1.17–6.24% w/w water showed no significant change in ρ_{MCC} (Table 3). Even though one would expect a small change in density because of the intrinsic density differences between water and microcrystalline cellulose, the air comparison pycnometer was not sensitive to the small change. Hence, the densities calculated do not reflect changes in water content.

References

Aklonis, J.J. and MacKnight, W.J., *Introduction to Polymer Viscoelasticity*, 2nd edn, Wiley, New York, 1983, Chap. 3.

American Pharmaceutical Association, *Handbook of Pharmaceutical Excipients*, Microcrystalline Cellulose, American Pharmaceutical Association, Washington, DC, 1986, pp. 53–55.

Barlow, A.J. and Lamb, J., The Viscoelastic Behavior of Lubricating Oils Under Cyclic Stress, *Proc. Royal Soc.*, A253 (1959) 52–69.

Beckman Instruments, Inc., *Instruction Manual for the Beckman Model 930 Air Comparison Pycnometer*, 1977.

Brook, D.P. and Marshall, K., Crushing Strength of Compressed Tablets I. Comparison of Testers. *J. Pharm. Sci.*, 57 (1968) 481–484.

Carstensen, J.T., *Pharmaceutics of Solids and Solid Dosage Forms*, Wiley, New York, 1977, pp. 135–177.

Danielson, D.W., Morehead, W.T. and Rippie, E.G., Unloading and Postcompression Viscoelastic Stress versus Strain Behavior of Pharmaceutical Solids. *J. Pharm. Sci.*, 72 (1983) 342–345.

David, S.T. and Augsburger, L.L., Flexure Test for Determination of Tablet Tensile Strength. *J. Pharm. Sci.*, 63 (1974) 933–936.

Durbetaki, A.J. and Quail, T.F., X-ray Diffraction and Fluorescence in the Analysis of Pharmaceutical Excipients. *Advances in X-ray Analysis*, vol. 25, Plenum, New York, (1982).

Fell, J.T. and Newton, J.M., The Tensile Strength of Lactose Tablets. *J. Pharm. Pharmacol.*, 20 (1968) 657–658.

Fell, J.T. and Newton, J.M., Determination of Tablet Strength by the Diametral-Compression Test. *J. Pharm. Sci.*, 59 (1970) 688–691.

Goodhart, F.W., Draper, J.R., Dancz, D. and Ninger, F., Evaluation of Tablet Breaking Strength Testers. *J. Pharm. Sci.*, 62 (1973) 297–304.

Heckel, R.W., Density-Pressure Relationships in Powder Compaction. *Trans. Met. Soc. AIME*, 221 (1961a) 671–675.

Heckel, R.W., An Analysis of Powder Compaction Phenomena. *Trans. Met. Soc. AIME*, 221 (1961b) 1001–1008.

Hiestand, E.N., Wells, J.E., Poet, C.B. and Ochs, J.F., Physical Processes of Tableting. *J. Pharm. Sci.*, 66 (1977) 510–519.

Hiestand, E.N. and Smith, D.P., Three Indices for Characterizing the Tableting Performance of Materials. *Advances in Ceramics, Forming of Ceramics.* Vol. 9, American Ceramic Society, 1984, pp. 47–57.

Jarosz, P.J. and Parrott, E.L., Factors Influencing Axial and Radial Tensile Strengths of Tablets. *J. Pharm. Sci.*, 71 (1982) 607–614.

Jetzer, W.E., Johnson, W.B. and Hiestand, E.N., Comparison of Two Different Experimental Procedures for Determining Compaction Parameters. *Int. J. Pharm.*, 26 (1985) 329–337.

Mashadi, A.B. and Newton, J.M., The Characterization of the Mechanical Properties of Microcrystalline Cellulose: A Fracture Approach. *J. Pharm. Pharmacol.*, 39 (1987) 961–965.

Nielsen, L.E., *Mechanical Properties of Polymers and Composites*, Vol. 2, Dekker, New York, 1974, Chap. 7.

Nyqvist, H. and Nicklasson, M., The Effect of Water Sorption on the Physical Properties of Tablets Containing Microcrystalline Cellulose. *Int. J. Pharm. Tech. Prod. Mfr.*, 4 (1983) 67–73.

Nystrom, C., Alex, W. and Malmquist, K., A New Approach to Tensile Strength Measurement of Tablets. *Acta Pharm. Suec.*, 14 (1977) 317–320.

Radebaugh, G.W. and Simonelli, A.P., Phenomenological Viscoelasticity of a Heterogeneous Pharmaceutical Semisolid. *J. Pharm. Sci.*, 72 (1983) 415–422.

Rippie, E.G. and Danielson, D.W., Viscoelastic Stress/Strain Behavior in Pharmaceutical Tablets: Analysis During Unloading and Postcompression Periods. *J. Pharm. Sci.*, 70 (1981) 476–482.

Zografi, G., Kontny, M.J., Yang, A.Y.S. and Brenner, G.S., Surface Area and Water Vapor Sorption of Microcrystalline Cellulose. *Int. J. Pharm.*, 18 (1984) 99–116.

Zografi, G. and Kontny, M.J., The Interactions of Water with Cellulose- and Starch-Derived Pharmaceutical Excipients. *Pharm. Res.*, 3 (1986) 187–194.

Zografi, G., States of Water Associated with Solids. *Drug Dev. Ind. Pharm.*, 14 (1988) 1905–1926.